Flow-Induced Flutter Instability of Functionally Graded Cantilever Pipe

Mostafa Rastgoo

Department of Materials Engineering, Sirjan Branch, Islamic Azad University, Sirjan, Iran.

Seyed Ahmad Fazelzadeh

Faculty of Mechanical Engineering, Shiraz University, Molla Sadra Ave, Shiraz, Iran, PO Box: 71345.

Malihe Eftekhari

Department of Mechanical Engineering, Yazd University, Yazd, I.R. Iran.

Mohammad Hosseini

Department of Mechanical Engineering, Sirjan University of Technology, 78137-33385 Sirjan, I.R., Iran.

(Received 23 November 2014; accepted 12 August 2015)

In this paper, the flutter characteristics of a functionally graded cantilever pipe conveying flow are presented. The functionally graded structural model is based on the classical thin-walled beam theory. The governing equations and boundary conditions are determined via Hamilton's variational principle. Then, the pipe partial differential equations are converted into a set of ordinary differential equations using the extended Galerkin method. Finally, having solved the resulting structural-fluid eigenvalue system of equations, we shed lights on the effects of volume fraction index and mass ratio on flutter speeds and frequencies. A validation of the selected result in comparison to the previous published literatures is also supplied.

1. INTRODUCTION

Cantilever pipes conveying fluids are of considerable interest and widely used in many applications. In the classification of dynamical systems, the cantilever pipe conveying fluid is found to be a non-conservative system, in which the work done by fluid on the pipe does not vanish. Therefore, in some oscillation cycles, the pipe will gain energy from the flow and may lose stability under high flow velocity by flutter. The transfer of energy between the flowing fluid and pipe was discussed by Benjamin.[1,2] Flutter of cantilevered continuous pipes conveying fluid was examined by Gregory and Païdoussis theoretically and experimentally.[3,4] Bert and Chen analyzed the vibration modes in orthotropic as well as isotropic pipes conveying fluid.[5] Païdoussis and Li reviewed and compiled the exhaustive literature available on the studies related to the dynamics of pipes conveying fluids.[6] Contributions by Païdoussis on dynamics of pipes conveying fluid are enormous and one can find a host of problems and solutions associated with fluid flowing through slender structures in these books.[7,8] Ryu et al. described the relationship between the eigenvalue branches and the corresponding unstable modes associated with flutter of cantilevered pipes conveying fluid.[9] Jayaraj et al. carried out elaborate parametric studies on various composite cylindrical shells conveying fluids.[10] For thin composite shells, they could predict the divergence as well as coupled mode flutter instabilities, and more importantly, established that the buckling mode due to the lowest critical velocity of the fluid coincides with the lowest natural frequency mode. Zhang et al. investigated the vibration characteristics of orthotropic cylindrical shells and tubes with initial tension and conveying fluid.[11,12] In order to investigate free vibration and buckling behavior of composite cylindrical shells conveying hot fluid, Kadoli and Ganesan presented a semi-analytical finite element method.[13]

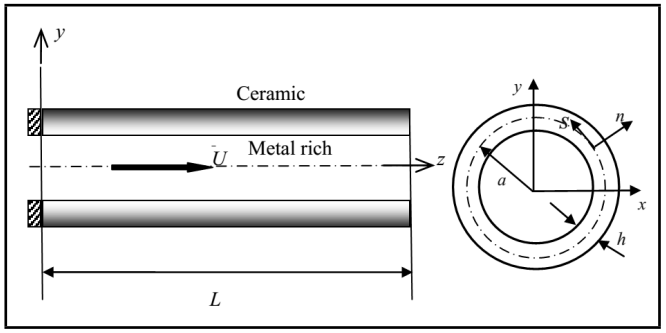

Figure 1. Pipe geometry and coordinate system.

In addition to the linear analysis, some nonlinear studies have dealt with cantilever pipes conveying fluid.[8,14] Yoon and Son investigated the effects of a tip mass and fluid flow on the dynamic behavior of a rotating cantilever pipe conveying fluid.[15] Modarres-Sadeghi and Païdoussis used the complete nonlinear model developed by Païdoussis[8] to evaluate the possibility of post-divergence instabilities in pipes supported at both ends.[16]

The concept of functionally graded material (FGM) was first introduced by a group of Japanese scientists to address the aggressive environment of thermal shock.[17] Since then, FGMs have received more and more attention in engineering communities, especially in applications for high-temperature mediums such as space planes, petrochemical plants, and nuclear reactors.[18–25] Sheng and Wang investigated the vibration of functionally graded cylindrical shells with flowing fluid. The first-order shear deformation theory was employed and the fluid velocity potential for the governing equation was developed.[26]

To the best of the author's knowledge, there are no studies dealing with the flutter analysis of FGM cantilever pipes conveying fluid. In the present paper, the completed model of

FGM cantilever pipes operating under a fluid flow pressure is developed. Furthermore, discussions about the combined effects of the fluid mass ratio and FGM volume fraction index on the flutter speed and frequency are presented.

2. PROBLEM DESCRIPTION

2.1. Pipe Geometrical Model

Consider a straight pipe conveying flow with velocity U of length L with a uniform thickness h and middle cord radius a in the $x-y$ plane as shown in Fig. 1. The origin of the Cartesian coordinate system is located at the geometric center of the pipe cross section. It should be remarked that (s,n,z) represents another local coordinates, where s and n, $-\frac{h}{2}\leq n\leq\frac{h}{2}$, are mid-line circumferential and thickness coordinates, respectively.

Components of the three-dimensional displacement vector are expressed as:[22]

$$u(x,y,z;t)=u_o(z;t);\qquad v(x,y,z;t)=v_o(z;t);$$
$$w(x,y,z;t)=\theta_x(z;t)\Big(y(s)-n\frac{dx}{ds}\Big)+\theta_y(z;t)\Big(x(s)+n\frac{dy}{ds}\Big); \tag{1}$$

where $u_o(z;t)$ and $v_o(z;t)$ are translations along the x and y axes, and $\theta_x(z;t)$ and $\theta_y(z;t)$ are rigid body rotations about the x and y axes. Based on the classical theory one can obtain

$$\theta_x(z;t)=-\frac{\partial v_o}{\partial z};\qquad \theta_y(z;t)=-\frac{\partial u_o}{\partial z}. \tag{2}$$

The position vector of a point $M(x,y,z)$ belonging to the deformed structure is:

$$\{R(x,y,z;t)\}=(x+u)\mathbf{i}+(y+v)\mathbf{j}+(z+w)\mathbf{k}. \tag{3}$$

By deriving the position vector, one obtains the velocity vector of an arbitrary point $M(x,y,z)$ of the pipe in the form,

$$\{\dot{R}\}=v_{px}\mathbf{i}+v_{py}\mathbf{j}+v_{pz}\mathbf{k}. \tag{4}$$

Their components are

$$v_{px}=\dot{u};\qquad v_{py}=\dot{v};\qquad v_{pz}=\dot{w}. \tag{5}$$

The velocity of the fluid is approximated as

$$\{v\}=v_{fx}\mathbf{i}+v_{fy}\mathbf{j}+v_{fz}\mathbf{k}; \tag{6}$$

where

$$v_{fx}=\dot{u}_o+U\frac{\partial u_o}{\partial z};$$
$$v_{fy}=\dot{v}_o+U\frac{\partial v_o}{\partial z};$$
$$v_{fz}=y_f\dot{\theta}_x+x_f\dot{\theta}_y+U. \tag{7}$$

Here, subscripts p and f describe the quantities associated with the pipe and fluid, respectively. The following strain displacement relation can be assumed as

$$\varepsilon_{zz}=\frac{\partial w}{\partial z}. \tag{8}$$

It is assumed that the original cross section of the pipe is preserved; therefore,[27]

$$\varepsilon_{xx}=\varepsilon_{yy}=\gamma_{xy}=0. \tag{9}$$

2.2. The FGM Model

On the macroscopic scale, FGMs are anisotropic, heterogeneous, and possess spatially continuous mechanical properties. For a ceramic/metal FGM model the material properties vary continuously across the pipe thickness according to the law given by Praveen and Reddy,[19]

$$P_{eff}=P_cV_c+P_mV_m;\qquad V_m=1-V_c; \tag{10}$$

where P_{eff} is material property, and V_m and V_c denote the volume fractions of metal and ceramic, respectively. Herein, subscripts m and c are quantities associated with metal and ceramic, respectively. The simple power law definition for the volume fraction of the ceramic-metal FGM is given as

$$V_c(n)=\left(\frac{n}{h}+\frac{1}{2}\right)^k; \tag{11}$$

where k, $0\leq k\leq\infty$, is the volume fraction parameter. This suggests that the material properties vary continuously from fully ceramic at the inner surface of the pipe to fully metal at the outer surface.

2.3. Constitutive Relations

Since the material used is isotropic, the corresponding elastic constitutive law adapted to the case of thin-walled structures is expressed as:[28]

$$\begin{bmatrix}\sigma_{ss}\\ \sigma_{zz}\end{bmatrix}=\begin{bmatrix}Q_{11}&Q_{12}\\ Q_{12}&Q_{11}\end{bmatrix}\begin{bmatrix}\varepsilon_{ss}\\ \varepsilon_{zz}\end{bmatrix}; \tag{12}$$

where

$$Q_{11}=\frac{E}{1-\nu^2};\qquad Q_{12}=\frac{E\nu}{1-\nu^2}. \tag{13}$$

Here, E and ν are the Young's modulus and Poisson's ratio, respectively.

3. GOVERNING EQUATIONS

The governing equations and boundary conditions can be derived via the extended Hamilton's principle for an open system with in-flow and out-flow of mass and momentum. This can be formulated as:[7]

$$\delta\int_{t_1}^{t_2}\ell_o\,dt\;-\int_{t_1}^{t_2}MU\big(\dot{R}_L+U\tau_L\big).\delta R_L\,dt=0;$$
$$\delta u_o=\delta v_o=0\qquad\text{at}\qquad t=t_1,t_2; \tag{14}$$

in which $\ell_o=T_o-V_o$ is the Lagrangian of the open system and T_o and V_o denote the kinetic and strain energies, respectively. Next, t_1 and t_2 are two arbitrary instants of time and δ is the variation operator. Further, R_L and τ_L are the position vector to a point on the free end of the pipe and tangential vector to the free end of the pipe, respectively.

The kinetic energy of the system is as follows:

$$T_o=T_p+T_f$$
$$=\frac{1}{2}\int_0^L\big(b_1\{\dot{R}\}.\{\dot{R}\}\big)dz+\frac{1}{2}\int_0^L M\{v_f\}.\{v_f\}\,dz; \tag{15}$$

where b_1 and M are mass per unit length of the pipe and fluid, respectively.

Also, the variation of strain energy based on the classical deformation theory of beams can be written as:

$$\delta V = -\int_0^L \left\{ \frac{\partial^2 M_y}{\partial z^2}\delta u_o + \frac{\partial^2 M_x}{\partial z^2}\delta v_o \right\} dz + \left[\frac{\partial M_y}{\partial z}\delta u_o + \frac{\partial M_x}{\partial z}\delta v_o - M_y \delta \frac{\partial u_o}{\partial z} - M_x \frac{\partial v_o}{\partial z} \right]\Bigg|_0^L; \quad (16)$$

where (M_x, M_y) are 1-D stress couples about x- and y-axis, respectively. Expressing 1-D stress couple in terms of 1-D displacement and substituting Eq. (15) and Eq. (16) into Eq. (14), using the integration by part, and noting the fact that the variations $(\delta u_o, \delta v_o)$ are independent and arbitrary, the equations of motion and the related boundary conditions can be obtained as,

$$\delta u_o : -a_{22}\frac{\partial^4 u_o}{\partial z^4} - MU^2\frac{\partial^2 u_o}{\partial z^2} - 2MU\frac{\partial^2 u_o}{\partial t \partial z} - (M+b_1)\frac{\partial^2 u_o}{\partial t^2} + (Mr^2+b_5+b_{15}+2b_{27})\frac{\partial^4 u_o}{\partial t^2 \partial z^2} = 0; \quad (17)$$

$$\delta v_o : -a_{33}\frac{\partial^4 v_o}{\partial z^4} - MU^2\frac{\partial^2 v_o}{\partial z^2} - 2MU\frac{\partial^2 v_o}{\partial t \partial z} - (M+b_1)\frac{\partial^2 v_o}{\partial t^2} + (Mr^2+b_4+b_{14}-2b_{23})\frac{\partial^4 v_o}{\partial t^2 \partial z^2} = 0; \quad (18)$$

where stiffness quantities $a_{ij} = a_{ji}$ and reduced mass terms b_i are defined in Librescu et al.[22] The corresponding boundary conditions result for a cantilever pipe are as:
at $z = 0$:

$$u_o = \frac{\partial u_o}{\partial z} = 0; \quad (19)$$

$$v_o = \frac{\partial v_o}{\partial z} = 0; \quad (20)$$

and at $z = L$:

$$\delta u_o : \; a_{22}\frac{\partial^3 u_o}{\partial z^3} - (Mr^2+b_5+b_{15}+2b_{27})\frac{\partial^3 u_o}{\partial t^2 \partial z} = 0; \quad (21)$$

$$\delta v_o : \; a_{33}\frac{\partial^3 v_o}{\partial z^3} - (Mr^2+b_4+b_{14}-2b_{23})\frac{\partial^3 v_o}{\partial t^2 \partial z} = 0; \quad (22)$$

$$\delta \frac{\partial u_o}{\partial z} : \; -a_{22}\frac{\partial^2 u_o}{\partial z^2} = 0; \quad (23)$$

$$\delta \frac{\partial v_o}{\partial z} : \; -a_{33}\frac{\partial^2 v_o}{\partial z^2} = 0; \quad (24)$$

where r is the internal gyration radius of the cross-sectional area of the pipe flow passage. It should be noted that the two partial differential equations (Eqs. (17) and (18)) are decouple. Therefore, because of symmetry for the cross section of the pipe with respect to the x and y axis, we can use only Eq. (17) with the associated boundary conditions (Eqs. (19), (21), and (23)).

For simplicity, the following dimensionless quantities are introduced:

$$\overline{u}_o = \frac{u_o}{h}; \quad \zeta = \frac{z}{L}; \quad \overline{r} = \frac{r}{L};$$

$$\beta_1 = \frac{b_1}{M+b_{1R}}; \; \beta_5 = \frac{b_5}{L^2(M+b_{1R})}; \; \beta_{15} = \frac{b_{15}}{L^2(M+b_{1R})};$$

$$\beta_{23} = \frac{b_{23}}{L^2(M+b_{1R})}; \quad \beta_{27} = \frac{b_{27}}{L^2(M+b_{1R})};$$

$$\tau = t\sqrt{\frac{a_{33R}}{(M+b_{1R})L^4}}; \quad \overline{\omega} = \omega\sqrt{\frac{(M+b_{1R})L^4}{a_{33R}}};$$

$$\mu = \frac{M}{M+b_{1R}}; \quad \overline{U} = U\sqrt{\frac{ML^2}{a_{33R}}}; \quad \overline{M}_y^T = \frac{M_y^T L^2}{a_{33R}h}. \quad (25)$$

Therefore, the dimensionless equation of motion is obtained as follows:

$$\frac{a_{22}}{a_{33R}}\overline{u}_o'''' + \overline{U}^2\overline{u}_o'' + 2\mu^{1/2}\overline{U}\dot{\overline{u}}_o' + (\mu+\beta_1)\ddot{\overline{u}}_o - (\mu\overline{r}^2+\beta_5+\beta_{15}+2\beta_{27})\ddot{\overline{u}}_o'' = 0; \quad (26)$$

where $\dot{(.)}$ and $(.)'$ denote the $\frac{\partial(.)}{\partial\tau}$ and $\frac{\partial(.)}{\partial\zeta}$, respectively. Herein, the subscript R denotes properties of the fully metallic pipe. Consequently, the dimensionless boundary condition is given below:
at $\zeta = 0$:

$$\overline{u}_o = \overline{u}_o' = 0; \quad (27)$$

and at $\zeta = 1$:

$$\frac{a_{22}}{a_{33R}}\overline{u}_o''' - (\mu\overline{r}^2+\beta_5+\beta_{15}+2\beta_{27})\ddot{\overline{u}}_o' = 0; \quad \frac{a_{22}}{a_{33R}}\overline{u}_o'' = 0. \quad (28)$$

4. SOLUTION METHODOLOGY

Due to the intricacy of the governing equations, the solution is sought using an approximate solution procedure. The partial differential Eq. (26) is converted into a set of linear ordinary differential equations according to the Galerkin's method. The non-dimensional lateral deflection $\overline{u}_o$ is expanded in a series of modes that satisfy the appropriate boundary conditions (Eqs. (27) and (28)). For a clamped-free pipe the following equation has been chosen

$$\overline{u}_o(\zeta,\tau) = \sum_{n=1}^{N}\Phi_n(\zeta)q_n(\tau); \quad (29)$$

where

$$\Phi(\zeta) = \cosh(\lambda_i\zeta) - \cos(\lambda_i\zeta) - \sigma_i\big(\sinh(\lambda_i\zeta) - \sin(\lambda_i\zeta)\big); \quad \sigma_i = \frac{\sinh(\lambda_i)-\sin(\lambda_i)}{\cosh(\lambda_i)+\cos(\lambda_i)}; \quad (30)$$

and λ_i can be obtained from the following equation:

$$\cosh(\lambda_i)\cos(\lambda_i) + 1 = 0; \quad (31)$$

where $\{q\} = \{q_1, q_2, \ldots, q_N\}^T$ is the overall vector of generalized coordinates and N is the number of used modes. Applying the extended Galerkin procedure on the governing equation (Eq. (26)), with the modal expansion (Eq. (29)), and using the orthogonal properties in the required integrations, the discretized form of the governing equation of motion for the cantilever pipe conveying flow is obtained as:

$$[M]\{\ddot{q}(\tau)\} + [G]\{\dot{q}(\tau)\} + [K]\{q(\tau)\} = 0; \quad (32)$$

where $[M]$, $[G]$, and $[K]$ denote the symmetric mass matrix, the non-symmetric damping matrix and the non-symmetric stiffness matrix, respectively, whose elements are given by

$$M_{ij} = (\mu+\beta_1)\delta_{ij} + (\mu\overline{r}^2+\beta_5+\beta_{15}+2\beta_{27})\vartheta_{ij};$$
$$G_{ij} = 2\mu^{1/2}\overline{U}\xi_{ij};$$
$$K_{ij} = \frac{a_{22}}{a_{33R}}\psi_{ij} + \overline{U}^2\zeta_{ij}; \quad (33)$$

Table 1. Material properties of metal (SUS304) and ceramic (Si3N4).[20]

Material	E (Pa)	ν	ρ (kg/m^3)
SUS304	207.79×10^9	0.32	8166
Si3N4	322.27×10^9	0.24	2370

where

$$\delta_{ij} = \begin{cases} 1 & i = j \\ 0 & i \neq j \end{cases};$$

$$\vartheta_{ij} = \begin{cases} \sigma_i\lambda_i\big(2+\sigma_i\lambda_i\big) & i = j \\ 4\frac{\lambda_i\lambda_j}{\lambda_i^2-\lambda_j^2}\Big((-1)^{i+j}\big(\sigma_j\lambda_i^3-\sigma_i\lambda_j^3\big)-\lambda_i\lambda_j\big(\sigma_i\lambda_i-\sigma_j\lambda_j\big)\Big); & \\ & i \neq j \end{cases}$$

$$\psi_{ij} = \begin{cases} \lambda_i^4 & i = j \\ 0 & i \neq j \end{cases};$$

$$\xi_{ij} = \begin{cases} 2 & i = j \\ 4\frac{\lambda_j^2}{\lambda_i^4-\lambda_j^4}\Big(\lambda_i^2-(-1)^{i+j}\lambda_j^2\Big) & i \neq j \end{cases};$$

$$\zeta_{ij} = \begin{cases} \sigma_i\lambda_i\big(2-\sigma_i\lambda_i\big) & i = j \\ 4\frac{\lambda_j^2(\sigma_i\lambda_i-\sigma_j\lambda_j)}{\lambda_i^4-\lambda_j^4}\Big((-1)^{i+j}\lambda_j^2+\lambda_i^2\Big) & i \neq j \end{cases}; \tag{34}$$

The Eq. (32) can be expressed in the first order variable form as

$$\{\dot{Z}(\tau)\} = [A]\{Z(\tau)\}; \tag{35}$$

where the state vector $\{Z(\tau)\}$ and the $2N \times 2N$ state matrix $[A]$ are defined as

$$\{Z(\tau)\} = \big\{\{q\}^T \quad \{\dot{q}\}^T\big\}^T; \tag{36}$$

$$[A] = \begin{bmatrix} [0] & [I] \\ -[M]^{-1}[K] & -[M]^{-1}[G] \end{bmatrix}; \tag{37}$$

while $[I]$ is the unitary matrix. Upon expressing $\{Z(\tau)\}$ in Eq. (35) as

$$\{Z(\tau)\} = \{X\}\exp(\overline{\Omega}\tau); \tag{38}$$

a standard eigenvalue problem is obtained

$$\big([A] - \overline{\Omega}[I]\big)\{X\} = 0; \tag{39}$$

where $\{X\}$ is a constant vector and $\overline{\Omega}$ is a constant-valued quantity. The eigenvalues or natural frequencies of the structural-fluid system can be obtained from the resulted equation. In general, the eigenvalues are complex; therefore,

$$\overline{\Omega}_n = \delta_n \pm i\omega_n; \qquad n = 1, 2, \ldots, N. \tag{40}$$

The nature of the dynamic response to any specified initial condition is strongly contingent on the sign of each δ_n. It should be noted that the real part of the eigenvalue, δ_n, is sometimes called the modal damping of the n^{th} mode, and ω_n is called the modal frequency. It is also possible to classify these motions from the stability standpoint. Typical response behavior can arise for positive, zero, and negative values of δ_n when ω_n is nonzero.

The convergent oscillations when $\delta_n < 0$ are termed dynamically stable and the divergent oscillations for $\delta_n > 0$ are dynamically unstable. The case of $\delta_n = 0$ represents the boundary between the two and is often called the "stability boundary."

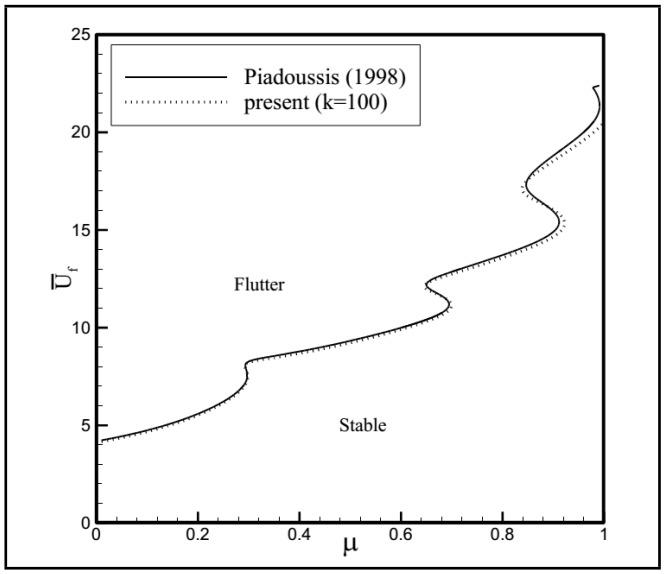

Figure 2. Validation of the flutter instability boundary of the fully metal cantilever FGM pipe, ($k = 100$).

5. NUMERICAL RESULTS

The functionally graded straight pipe, considered as a thin-walled beam, has a uniform circular cross section with the following geometric characteristics,[22]

$$a = 0.127 \text{ m}; \quad L = 2.032 \text{ m}; \quad h = 0.01 \text{ m}. \tag{41}$$

The numerical study is carried out to supply information on the flutter boundary with different material properties. Also, the first six terms of mode expansion in Galerkin's procedure are used in the numerical simulations.

The functionally graded materials are composed of silicon nitride and stainless steel, referred to as Si3N4/SUS304 and their properties are listed in Table 1 (from Reddy and Chin[20]).

As the first step, for a fully metal case ($k = 100$) that exposes an isotropic property, the accuracy of the method is verified against those reported by Païdoussis[7] and good agreement is obtained as shown in Fig. 2. As shown in this figure, the critical flow velocities have few differences from those presented by Païdoussis. This deviation is due to the rotary inertia term that is considered here in Eq. (26).

Throughout the numerical simulation the following dimensionless frequency parameters are considered

$$\overline{\omega}_i = \frac{\omega_i}{\hat{\omega}_1}; \qquad i = 1, 2, \ldots, N. \tag{42}$$

where $\hat{\omega}_1$ is the first natural frequency of the fully metallic pipe without fluid flow. In the obtained results, $\overline{U}_f$ and $\overline{\omega}_f$ are non-dimensional flutter velocity fluid flow and non-dimensional flutter frequency parameters, respectively.

Figure 3 shows the influence of the non-dimensional fluid mass ratio on the flutter velocities for various volume fraction indexes of FGMs.

It is found out that the cantilever pipe is stable for the flow velocities lower than the critical value and is unstable over the critical value. As it is shown in this figure, increasing the ceramic constituent of the FGMs pipe increases the non-dimensional critical flow velocities. This improves the cantilever pipe dynamic behavior due to the expansion of the stability domain. This is due to the fact that the increase of the ceramic constituent of the FGMs pipe increases the bending

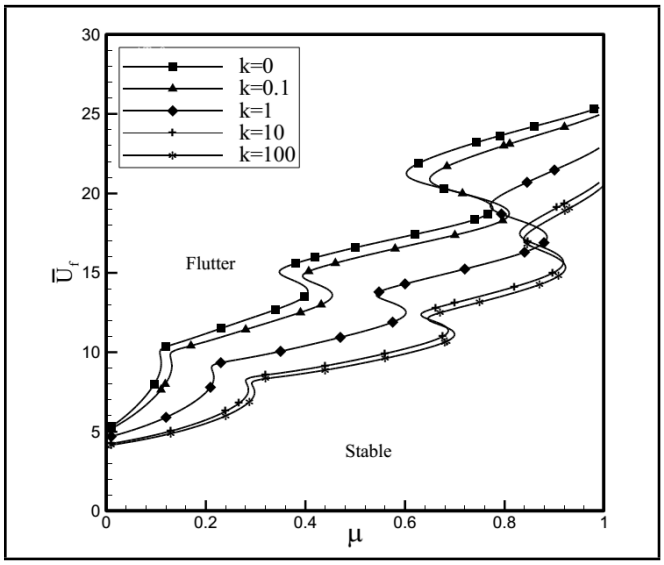

Figure 3. Critical flutter velocities of the cantilever FGM pipe in terms of mass ratio (μ) for selected values of volume fraction index (k).

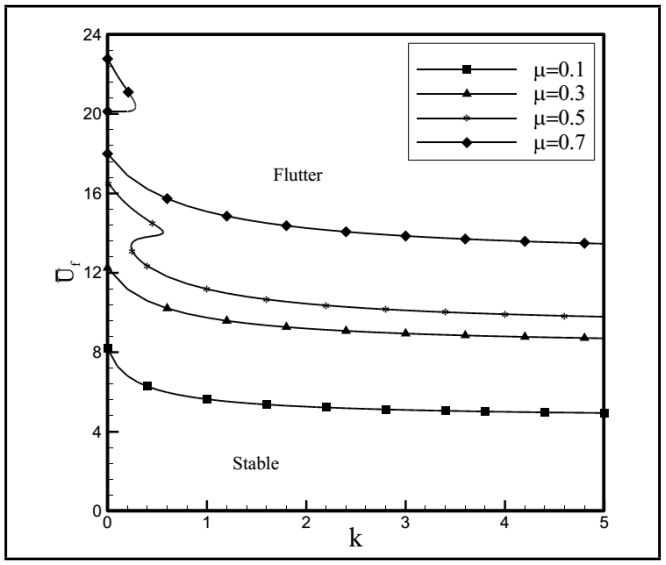

Figure 5. Critical flutter velocities of the cantilever FGM pipe in terms of volume fraction index (k) for selected values of mass ratios (μ).

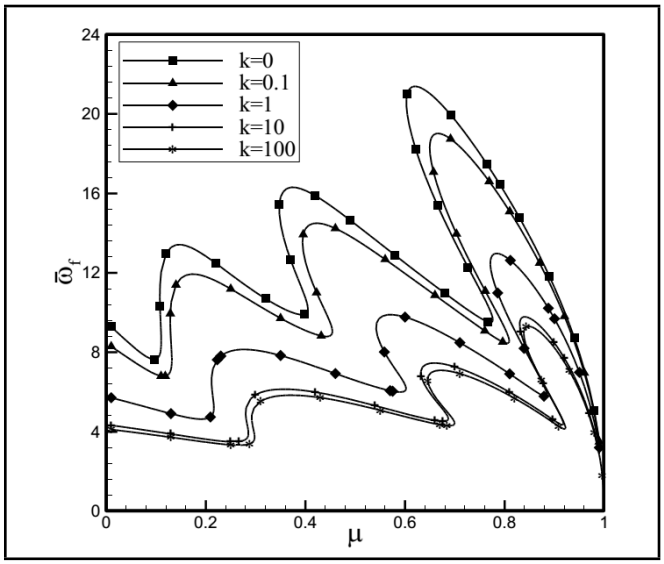

Figure 4. Critical flutter frequencies of the cantilever FGM pipe in terms of mass ratio (μ) for selected values of volume fraction index (k).

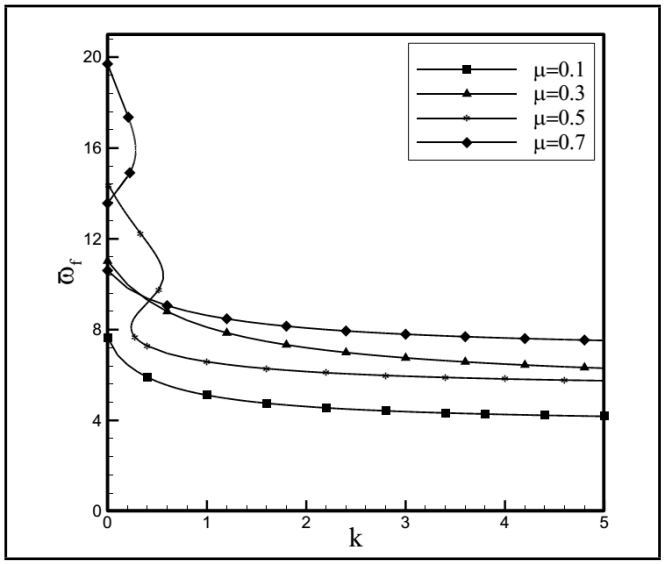

Figure 6. Critical flutter frequencies of the cantilever FGM pipe in terms of volume fraction index (k) for selected values of mass ratios (μ).

stiffness of the whole pipe. Therefore, the stability domain of the pipe expands more than the other in the same condition, but with higher volume fraction index.

In Fig. 4, the corresponding non-dimensional frequency parameters are presented vs. the mass ratios. As expected, an increase in volume fraction indexes causes the flutter frequency parameter to be reduced.

The non-dimensional flow velocities and corresponding frequency parameters as a function of volume fraction index are plotted in Fig. 5 and Fig. 6, respectively.

The non-dimensional flow velocity and frequency parameter vary more gradually beyond $k \approx 5$. Increasing the volume fraction of the ceramic base increases the flutter frequency. Although the ceramic constituent part tends to increase the stability zones, it may yield premature failure by fatigue, which is an adverse effect due to the increase in flutter frequencies.

6. CONCLUSIONS

The stability analysis for a cantilever FGM pipe conveying fluid flow is investigated. Moreover, the analysis is performed, and the influence of some physical parameters of the system, such as mean flow velocity, mass ratios, and volume fraction index of FGM pipes on the regions of stability are discussed. Mass ratios and volume fraction index of FGM pipes imposed a noticeable effect on the non-dimensional flutter velocities and on the flutter frequency parameters. An increase in the volume fraction index results in the condensation of stable domains and so leads to a reduction of flutter frequency parameters.

REFERENCES

[1] Benjamin, T. B. Dynamics of a system of articulated pipes conveying fluid. I. Theory, *Proceedings of the Royal Society of London Series A*, **261**, 457–486, (1961). https://dx.doi.org/10.1098/rspa.1961.0090

[2] Benjamin, T. B. Dynamics of a system of articulated pipes conveying fluid. II. Experiments, *Proceedings of the Royal Society of London Series A*, **261**, 487–499, (1961). https://dx.doi.org/10.1098/rspa.1961.0091

[3] Gregory, R. W. and Païdoussis, M. P. Unstable oscillation of tubular cantilevers conveying fluid. I. Theory, *Proceedings of the Royal Society of London Series A*, **293**, 512–527, (1966). https://dx.doi.org/10.1098/rspa.1966.0187

[4] Gregory, R. W. and Païdoussis, M. P. Unstable oscillation of tubular cantilevers conveying fluid. II. Experiments, *Proceedings of the Royal Society of London Series A*, **293**, 528–542, (1966). https://dx.doi.org/10.1098/rspa.1966.0188

[5] Bert, C. W. and Chen, T. L. C. Wave propagation in fluid conveying piping constructed of composite material, *Journal of Pressure Vessel Technology*, **178**, 178–84, (1975). https://dx.doi.org/10.1115/1.3454292

[6] Païdoussis, M. P. and Li, G. X. Pipes conveying fluid: a model dynamic problem, *Journal of Fluids and Structures*, **7**, 137–204, (1993). https://dx.doi.org/10.1006/jfls.1993.1011

[7] Païdoussis, M. P. *Fluid-Structure Interactions: Slender Structures and Axial Flow*, vol. 1, Academic Press, London, (1998).

[8] Païdoussis, M. P. *Fluid-Structure Interactions: Slender Structures and Axial Flow*, vol. 2, Elsevier Academic Press, London, (2004).

[9] Ryu, S., Sugiyama, Y., and Ryu, B. Eigenvalue branches and modes for flutter of cantilevered pipes conveying fluid, *Computers and Structures*, **80**, 1231–1241, (2002). https://dx.doi.org/10.1016/S0045-7949(02)00083-4

[10] Jayaraj, K., Ganesan, N., and Chandramouli, P. A semi-analytical coupled finite element formulation for composite shells conveying fluids, *Journal of Sound and Vibration*, **258**, 287–307, (2002). https://dx.doi.org/10.1006/jsvi.2002.5176

[11] Zhang, Y. L., Gorman, D. G., and Reese, J. M. A finite element method for modelling the vibration of initially tensioned thin-walled orthotropic cylindrical tubes conveying fluid, *Journal of Sound and Vibration*, **245**, 93–112, (2001). https://dx.doi.org/10.1006/jsvi.2000.3554

[12] Zhang, Y. L., Reese, J. M., and Gorman, D. G. Initially tensioned orthotropic cylindrical shells conveying fluid: A vibration analysis, *Journal of Fluids and Structures*, **16** (1), 53–70, (2002). https://dx.doi.org/10.1006/jfls.2001.0409

[13] Kadoli, R. and Ganesan, N. Free vibration and buckling analysis of composite cylindrical shells conveying hot fluid, *Composite Structures*, **60**, 19–32, (2003). https://dx.doi.org/10.1016/S0263-8223(02)00313-6

[14] Wadham-Gagnon, M., Païdoussis, M. P., and Semler, C. Dynamics of cantilevered pipes conveying fluid. Part 1: Nonlinear equations of three-dimensional motion, *Journal of Fluids and Structures*, **23**, 545–567, (2007).

[15] Yoon, H. and Son, I. Dynamic response of rotating flexible cantilever pipe conveying fluid with tip mass, International *Journal of Mechanical Sciences,* **49**, 878–887, (2007). https://dx.doi.org/10.1016/j.jfluidstructs.2006.10.006

[16] Modarres-Sadeghi, Y. and Païdoussis, M. P. Nonlinear dynamics of extensible fluid-conveying pipes, supported at both ends, *Journal of Fluids and Structures*, **25**, 535–543, (2009). https://dx.doi.org/10.1016/j.jfluidstructs.2008.09.005

[17] Yamanouchi, M., Koizumi, M., Hirai, T., and Shiota, I. On the design of functionally gradient materials, *Proceeding of the First International Symposium on Functionally Gradient Materials*, 5–10, Sendai, Japan, (1990).

[18] Pindera, M. J., Aboudi, J., and Arnold, S. M. Limitations of the uncoupled, RVE-based micromechanical approach in the analysis of functionally graded composites, *Mechanics of Materials*, **20**, 77–94, (1995). https://dx.doi.org/10.1016/0167-6636(94)00052-2

[19] Praveen, G. N. and Reddy, J. N. Nonlinear transient thermoelastic analysis of functionally graded ceramic metal plates, *International Journal of Solids and Structures*, **35**, 4457–4476, (1998). https://dx.doi.org/10.1016/S0020-7683(97)00253-9

[20] Reddy, J. N. and Chin, C. D. Thermomechanical analysis of functionally graded cylinders and plates, *Journal of Thermal Stresses*, **21**, 593–629, (1998). https://dx.doi.org/10.1080/01495739808956165

[21] Loy, C. T., Lam, K. Y. and Reddy, J. N. Vibration of functionally graded cylindrical shells, *International Journal of Mechanical Sciences*, **41**, 309–324, (1999). https://dx.doi.org/10.1016/S0020-7403(98)00054-X

[22] Librescu, L., Oh, S. Y., and Song, O. Thin-walled beams made of functionally graded materials and operating in a high temperature environment: Vibration and stability, *Journal of Thermal Stresses*, **28**, 649–712, (2005). https://dx.doi.org/10.1080/01495730590934038

[23] Woo, J., Meguid, S. A., Stranart, J. C., and Liew, K. M. Thermomechanical postbuckling analysis of moderately thick functionally graded plates and shallow shells, *International Journal of Mechanical Sciences*, **47**, 1147–1171, (2005). https://dx.doi.org/10.1016/j.ijmecsci.2005.04.008

[24] Arciniega, R. A. and Reddy, J. N. Large deformation analysis of functionally graded shells, *International Journal of Solids and Structures*, **44**, 2036–2052, (2007). https://dx.doi.org/10.1016/j.ijsolstr.2006.08.035

[25] Fazelzadeh, S. A. and Hosseini, M. Aerothermoelastic behavior of supersonic rotating thin-walled beams made of functionally graded materials, *Journal of Fluids and Structures*, **23**, 1251–1264, (2007). https://dx.doi.org/10.1016/j.jfluidstructs.2007.06.006

[26] Sheng, G. G. and Wang, X. Thermomechanical vibration analysis of a functionally graded shell with flowing fluid, *European Journal of Mechanics — A/Solids*, **27**, 1075–1087, (2008). https://dx.doi.org/10.1016/j.euromechsol.2008.02.003

[27] Qin, Z. and Librescu, L. On a shear-deformable theory of anisotropic thin-walled beams: further contribution and validations, *Composite Structures*, **56**, 345–358, (2002). https://dx.doi.org/10.1016/S0263-8223(02)00019-3

[28] Noda, N., Hetnarski, R. B., and Tanigawa, Y. *Thermal Stresses*, Second edition, Taylor & Francis, New York, (2003).